

Brownian non-Gaussian polymer diffusion in non-static media

Xiao Zhang,¹ Heng Wang,¹ and Weihua Deng¹

School of Mathematics and Statistics, State Key Laboratory of Natural Product Chemistry, Lanzhou University, Lanzhou 730000, China.

(*Electronic mail: dengwh@lzu.edu.cn)

(Dated: 21 October 2024)

In nature, essentially almost all the particles move irregularly in non-static media. With the advance of observation techniques, various kinds of new dynamical phenomena are detected, e.g., Brownian non-Gaussian diffusion. This paper focuses on the dynamical behavior of the center of mass (CM) of polymer in non-static media and investigates the effect of polymer size fluctuations on the diffusion behavior. Firstly, we establish a diffusing diffusivity model for polymer size fluctuations, linking the polymer size variation to the birth and death process, and introduce co-moving and physical coordinate systems to characterize the position of the CM for polymer in non-static media. Next, the important statistical quantities for the CM diffusing diffusivity model in non-static media, such as mean square displacement (MSD) and kurtosis, are obtained by adopting the subordinate process approach, and the long-time asymptotic behavior of the MSD in the media of different types is specifically analyzed. Finally, the bivariate Fokker-Planck equation and the Feynman-Kac equation corresponding to the diffusing diffusivity model are detailedly derived and solved through the deep BSDE method to confirm the correctness of the derived equations.

In a non-static media, the medium itself is in a state of motion, thereby affecting the movement of particles. When the motion mode of the particle is random walk, through the change of volume in the non-static medium and in combination with the classical Chapman-Kolmogorov equation¹⁻³, the corresponding diffusion equation and the Langevin equation⁴ can be derived to describe the diffusion behavior of particles in different media. In order to investigate the particle motion in the non-static medium, it is necessary for us to introduce the comoving coordinate system. By establishing the relationship between the comoving coordinate system and the physical coordinate system⁵⁻⁸, the tools for researching the random model in the static medium can be employed to explore the diffusion behavior of the particles in the non-static medium. As for the diffusion behavior of Brownian non-Gaussian⁹⁻¹¹, which is experimentally discovered, it has been found that the generalized grey Brownian motion¹² and the diffusing diffusivity model¹³ are adopted to study it. In recent years, Brownian non-Gaussian diffusion phenomena have been frequently observed in biological systems^{14,15}. The present paper focuses on the non-Gaussian diffusion behaviour of the polymer CM in the non-static state, where the movement of CM is not only affected by the motion of the medium, but also by the Brownian motion of the polymer as a whole and the fluctuation on the number of polymer monomers.

diation and matter-dominated expansion is represented by a power law scaling factor¹⁷, whereas the expansion controlled by dark energy is determined by an exponential scaling factor^{17,18}. In developmental biology¹⁹⁻²², the formation of biological structures is impacted by the tissues and organs that accompany the growth process. The non-static medium itself is in motion, implicating the movement of the particle. Continuous-time random walks⁶ (CTRW) and Lévy walks^{7,8} with coupled time and space and finite velocity are central stochastic models for describing non-static diffusion mechanisms. Alternatively, the anomalous diffusion of the particle in a non-static medium is explored within the framework of Langevin's equation²³.

Numerous different complex and irregular systems are generally accompanied by a variety of diffusion phenomena. To be specific, this diffusion is manifested in the MSD of the motion of the particle, i.e., $\langle x^2(t) \rangle = \int_{-\infty}^{\infty} x^2 P(x, t) dx$ exhibits various relations $\langle x^2(t) \rangle \sim t^a$. As a general rule, $a > 1$ and $0 < a < 1$ respectively correspond to 2 types of diffusion, i.e., superdiffusion and subdiffusion. With regard to anomalous diffusion, the models that we typically utilize to investigate are: the generalized Langevin equation with power law or exponential memory kernel²⁴, the fractional Brownian motion²⁵ (FBM), the CTRW model²⁶⁻²⁸, α -stable subordination process²⁹, and the Lévy walk model³⁰, etc. For the case of $\langle x^2(t) \rangle \sim t$, previously it was viewed as a normal Brownian Gaussian diffusion³¹⁻³³.

Extensive exploration and experiments on natural phenomena have led to the discovery of a new kind of diffusion phenomenon. This phenomenon manifests itself as a linear relationship for the MSD of the particle with respect to time, analogous to normal Brownian diffusion, yet the particle's probability density function (PDF) is not Gaussian distribution. The Granick group initially employs single-particle tracking experiments, involving colloidal particle motion on a phospholipid bilayer¹⁰ and entanglement in the F-actin network⁹, both of which reveal this new diffusion phenomenon. Subsequently this phenomenon has been called Brownian non-

I. INTRODUCTION

The majority of previous diffusion processes have been analyzed in static media, i.e., when the particle is not in motion, the position of the particle does not change with time. However, in nature, the phenomena occurring in non-static homogeneous media are exceedingly ubiquitous. In cosmology¹⁶, cosmic rays diffuse in an expanding universe, where the ra-

Gaussian diffusion¹¹ and has been observed in a variety of systems. Predominantly, it is seen in physical and biological systems, such as the random motion of tracer particles in polymer suspensions^{14,15}, the diffusion of nanoparticles in nanopillar arrays³⁹, the individual dynamic behavior in heterogeneous populations of parasitic nematodes⁴⁰, and the diffusion of RNA molecules in living *E. coli* and yeast cells³⁴. At a microscopic level, identifying potential mechanisms can help explain experimental phenomena. The literature⁴¹ proposes polymerisation and depolymerisation of monomers in polymers, providing a basis for studying this anomalous diffusion. The literatures^{42,43} consider polymers in contact with a chemostatted monomer bath. By changing the monomer concentration in the monomer bath, polymers change from finite growth to infinite growth (the size fluctuations of polymers are characterized by a “birth and death process”), explaining the return of the polymer CM from initial Brownian non-Gaussian diffusion to normal diffusion. To fill this gap in such diffusion in non-static media, we generalize the diffusion model to non-static media.

Numerous experiments involve the analysis of trajectories of tagged particles with distinct non-Gaussian diffusion origins. Two main strategies of studying non-Gaussian diffusion due to random diffusion coefficients are the generalized grey Brownian motion (ggBM) and the diffusing diffusivity (DD) model. The first ggBM is defined by the stochastic equation¹²

$$x(t) = \sqrt{2DB}(t), \quad (1)$$

in which $x(t)$ denotes the particle trajectory, and $B(t) = \int_0^t \xi(t)dt$ is the standard Wiener process (Brownian motion). The diffusion coefficient D is a random variable independent of time and comes from the distribution $p(D)$. The diffusion of particles with random diffusion coefficients in the ggBM model within steady and complex environments is concordant with the diffusion examined by the superstatistical approach¹³. The second stochastic model is the DD model, as defined by the overdamped Langevin equation¹³

$$\frac{dx(t)}{dt} = \sqrt{2D(t)}\xi(t). \quad (2)$$

In this model, the diffusion coefficient $D(t)$ is a time dependent random variable or stochastic process. The evolution of the motion of the particle undergoes both the temporal continuity of its own diffusion coefficient and the overall randomness of Brownian motion in the DD model. While the DD model is consistent with the results of the superstatistical approach for short time (less than $D(t)$ autocorrelation time), beyond a characteristic time scale (greater than $D(t)$ autocorrelation time) the evolution trend of the particles gradually turns from non-Gaussian to Gaussian diffusion. More models include exponentially distributed FBM, random diffusivity for scaled Brownian motion, diffusing diffusivity FBM, and Brownian motion in quenched disordered landscapes^{34–38}.

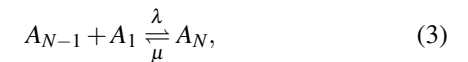
In this paper, we investigate a broader DD process that probes the diffusion behavior of the CM of polymer in a non-static media. In this process, the diffusion coefficient $D(t)$ is a “birth and death process” related to the number of polymer

monomers, and $D(t)$ is subordinated to Brownian motion as a stochastic process. In Section II, we introduce the stochastic process $N(t)$ with respect to the number of polymer monomers and calculate the steady-state distribution of the stochastic process $N(t)$. In Section III, the DD model in a non-static media is presented to discuss the kinetic behavior of the CM of polymer. Statistical quantities related to the position of the CM are individually obtained and simulated in different types of media. We derive the bivariate Fokker-Planck equation for the PDF of the CM in Section IV and get the corresponding Feynman-Kac equation of the DD model. In Section V, we solve the equations derived in Section IV using the deep BSDE method and validate it (also the correctness of the equation) by simulations with the Monte Carlo method. Important results are summarized and discussed in the last section.

II. POLYMERIZATION AND DEPOLYMERIZATION PROCESS

Polymers are high-molecular compounds formed by the linkage of monomers through reaction mechanisms like polycondensation or ring-opening polymerization, resulting in polymer chains. The molecular weight of polymers is generally quite high and can reach thousands or even millions of molecules. Polymer molecules can bond with other to form a mesh structure, which endows the material with special properties such as elasticity and toughness. As such, polymers have a broad range of applications, notably in the arenas of plastics, rubber, coatings, fibers, and electronic devices.

Suppose that a polymer A_N consists of N monomers A_1 in an environment with infinite monomers. The increase (polymerization) and decrease (depolymerization) of monomers at both ends of the polymer A_N is hereby depicted by the chemical reaction⁴⁴



in which λ and μ are the polymerization and depolymerization rates, respectively, and neither λ nor μ is dependent on the number of polymer monomers. Likewise, the description of this chemical reaction process can be achieved through the $M/M/1/\infty$ model in queueing theory. Here, the first M and the second M respectively represent the Markov arrival time and the Markov service completion time, both following the exponential distribution. The 1 indicates only a single service desk, while ∞ signifies an unlimited number of customers. Corresponding to the above chemical reaction (3), a linear polymer A_N , with polymerization and depolymerization rates obeying exponential distributions respectively with parameters λ and μ , reacts in a monomer infinite environment.

This chemical reaction can be considered as a Markov process $\{N(t), t > 0\}$, in which $N(t)$ represents the number of monomers of polymer at t . From the chemical reaction (3), it is obvious that there is a fluctuation in the number of polymer monomers, where A_N occurs between neighboring states. Therefore, $N(t)$ can be treated as a birth and death process,

taking the polymerization and depolymerization processes as “birth” and “death”.

The alteration in the number of polymer monomers is presented for short τ durations, and the probabilities of monomer polymerization and depolymerization within the $(t, t + \tau)$ time period are shown in Table I. The probabilities of monomer polymerization and depolymerization in a brief τ time period are $\int_0^\tau \lambda e^{-\lambda t'} dt'$ and $\int_0^\tau \mu e^{-\mu t'} dt'$, respectively. As the amount of monomers varies between adjacent states, there are three cases for the number of polymer monomers at t time, i.e., $n - 1$, n , and $n + 1$. Hence, the probability that the polymer has n monomers at the time $t + \tau$ can be represented as four mutually exclusive cases. In accordance with the full probability formula, at the initial moment $t = 0$ and $n = n_0$, $P_N(n, t + \tau | n_0)$ can be represented as

$$\begin{aligned} P_N(n, t + \tau | n_0) &= P_N(n + 1, t | n_0)[(1 - \lambda\tau + o(\tau))(\mu\tau + o(\tau))] \\ &+ P_N(n - 1, t | n_0)[(\lambda\tau + o(\tau))(1 - \mu\tau + o(\tau))] \quad (4) \\ &+ P_N(n, t | n_0)[(1 - \lambda\tau + o(\tau))(1 - \mu\tau + o(\tau)) \\ &+ (\lambda\tau + o(\tau))(\mu\tau + o(\tau))] + o(\tau). \end{aligned}$$

After collecting like terms in (4) and dividing by τ , as $\tau \rightarrow 0$, omitting the higher-order terms, (4) can be written as the forward Kolmogorov equation

$$\begin{aligned} \frac{\partial}{\partial t} P_N(n, t | n_0) &= \mu P_N(n + 1, t | n_0) - (\mu + \lambda) P_N(n, t | n_0) \\ &+ \lambda P_N(n - 1, t | n_0) \quad n \geq 1, \\ \frac{\partial}{\partial t} P_N(0, t | n_0) &= \mu P_N(1, t | n_0) - \lambda P_N(0, t | n_0). \end{aligned} \quad (5)$$

Beside that, it is essential to obtain the steady-state distribution of this process $P^*(n) = \lim_{t \rightarrow \infty} P_N(n, t | n_0)$; the existence of $P^*(n)$ requires that the birth process is ergodic⁴⁵, i.e., it satisfies the requirement

$$\sum_{i=1}^{\infty} \prod_{n=1}^i \frac{\mu_n}{\lambda_n} = \infty$$

and

$$\sum_{i=1}^{\infty} \prod_{n=1}^i \frac{\lambda_{n-1}}{\mu_n} < \infty.$$

In the context of the birth and death process discussed, the polymerization rate λ and the dissociation rate μ have no dependence on the number of monomers. The process features a steady-state distribution $P^*(n)$ given that $\lambda < \mu$, and it can be obtained by setting equation (5) with $\partial_t P_N(n, t | n_0) = 0$, i.e., to solve

$$\begin{aligned} 0 &= \lambda P^*(n - 1) - (\mu + \lambda) P^*(n) + \mu P^*(n + 1) \quad n \geq 1, \quad (6) \\ 0 &= \mu P^*(1) - \lambda P^*(0). \end{aligned}$$

By means of recursion, it can be got that $\sum_{n=0}^{\infty} P^*(n) = \sum_{n=0}^{\infty} \left(\frac{\lambda}{\mu}\right)^n P^*(0) = 1$, so the steady-state distribution is

$P^*(n) = \left(1 - \frac{\lambda}{\mu}\right) \left(\frac{\lambda}{\mu}\right)^n$. $P^*(n)$ is also available through the specific distribution as $t \rightarrow \infty$ obtained from the literature⁴⁶. Based on the autocorrelation time scale⁴³ η of the stochastic process $N(t)$, the asymptotic approximation of $P_N(n, t | n_0)$ is categorized into two scenarios in the subsequent study, specifically, taking $t \ll \eta$ and $t \gg \eta$, which are asymptotic to $P_N(n, t | n_0) \sim \delta_{n, n_0}$ and $P_N(n, t' | n_0) \sim P^*(n)$.

III. DD MODEL IN NON-STATIC MEDIA

Taking into account the position for the CM of polymer in three dimensions, it is customary to represent the position in static and non-static media separately using co-moving coordinate and physical coordinate⁴, as detailed below,

$$\bar{\mathbf{r}} = a(t)\mathbf{r}, \quad (7)$$

whereby $\bar{\mathbf{r}} = (\bar{x}, \bar{y}, \bar{z})$ is the physical coordinate, $\mathbf{r} = (x, y, z)$ is the co-moving coordinate, and $a(t)$ is the scale factor with $a(0) = 1$.

We first consider Brownian motion in non-static media, and there are two ways to obtain its corresponding Langevin equation: The CTRW model in non-static media can be used to describe Brownian motion in non-static media^{5,6}; When the motion of the particle is random walk, combining the change of the volume in the non-static medium and the classical Chapman-Kolmogorov equations results in the corresponding Fokker-Planck equation and Langevin equation⁴. Consistent with the Stokes-Einstein relationship in polymer physics^{47,48}, the diffusion coefficient is proportional to the inverse of the hydrodynamic radius of the polymer, that is, $D(N) \sim 1/N^\beta$. Here it is deemed that the diffusion coefficient⁴³ of a polymer with $N = n$ monomers is $D(n) = D_0/(n + n_{\min})^\beta$, where D_0 is the diffusion coefficient specific to the polymer monomer, n_{\min} is the smallest conformation of the polymer, and the exponent β is determined based on the polymer model^{41,47}. Particularly, the three values 1, 1/2, and 2 of β , respectively, correspond to the Zimm, Rouse, and Reptation models of polymers. Combining the analysis of the polymer depolymerization and polymerization processes in Section II and the definition of the diffusion coefficient, it becomes evident that $D(n(t))$ is a stochastic process. Suppose that the evolution of the number of polymer monomers is not affected by the non-static medium, but the CM of polymer position follows Brownian motion, affected by the size fluctuation in the non-static media. Then the motion of the CM can be represented by DD model^{13,43,49} as

$$d\bar{\mathbf{r}}(t) = \frac{a'(t)}{a(t)} \bar{\mathbf{r}}(t) dt + \sqrt{2D(n(t))} d\mathbf{B}(t), \quad (8)$$

whereby $\bar{\mathbf{r}}(t) = (\bar{x}(t), \bar{y}(t), \bar{z}(t))$, $\mathbf{B}(t)$ is a 3-dimensional Wiener process (Brownian motion), and the diffusion coefficient $D(n(t)) = D_0/(n(t) + n_{\min})^\beta$. The diffusion coefficient is related to the polymer size, and it can be seen that $\bar{\mathbf{r}}(t)$ is a composite stochastic process. With polymer size fluctuations, given $n(t)$, the PDF $P(\bar{\mathbf{r}}, t | n(t))$ for CM position satisfies the

TABLE I. Change for the number of monomers in $(t, t + \tau)$.

	The reaction in τ	Probability
$\mathbb{P}(N(t + \tau) - N(t) = 1 N(t) = k)$	A monomer polymerization	$\lambda \tau + o(\tau)$
$\mathbb{P}(N(t + \tau) - N(t) = -1 N(t) = k)$	A monomer depolymerization	$\mu \tau + o(\tau)$
$\mathbb{P}(N(t + \tau) - N(t) > 1 N(t) = k)$	Multiple monomers polymerization	$o(\tau)$
$\mathbb{P}(N(t + \tau) - N(t) < -1 N(t) = k)$	Multiple monomers depolymerization	$o(\tau)$
$\mathbb{P}(N(t + \tau) - N(t) = 0 N(t) = k)$	No polymerization and depolymerization	$(1 - \lambda \tau + o(\tau))(1 - \mu \tau + o(\tau))$

general diffusion equation

$$\frac{\partial P(\bar{\mathbf{r}}, t | n(t))}{\partial t} = -\frac{a'(t)}{a(t)} \nabla_{\bar{\mathbf{r}}} \cdot (\bar{\mathbf{r}} P(\bar{\mathbf{r}}, t | n(t))) + \frac{D_0}{(n(t) + n_{\min})^\beta} \nabla_{\bar{\mathbf{r}}}^2 P(\bar{\mathbf{r}}, t | n(t)). \quad (9)$$

Adopting the processing steps of the literature⁴, the diffusion equation (9) can be transformed into the co-moving coordinate system to investigate. Letting $P_{\mathbf{r}}(\mathbf{r}, t | n(t)) = P(\bar{\mathbf{r}} = a(t)\mathbf{r}, t | n(t))$, then one can get

$$\frac{\partial P_{\mathbf{r}}(\mathbf{r}, t | n(t))}{\partial t} = \frac{D(n(t))}{a^2(t)} \nabla_{\mathbf{r}}^2 P_{\mathbf{r}}(\mathbf{r}, t | n(t)) - \frac{a'(t)}{a(t)} P_{\mathbf{r}}(\mathbf{r}, t | n(t)). \quad (10)$$

Further denote the corresponding part of $P(\bar{\mathbf{r}}, t | n(t))$ in co-moving space as $W(\mathbf{r}, t | n(t))$, the PDF of the CM at position \mathbf{x} and time t with provided $n(t)$. The relationship for PDFs in the two coordinate systems is as follows

$$P(\bar{\mathbf{r}}, t | n(t)) = \frac{W(\frac{\bar{\mathbf{r}}}{a(t)}, t | n(t))}{a(t)}. \quad (11)$$

It is evident that $P_{\mathbf{r}}(\mathbf{r}, t | n(t)) = W(\mathbf{r}, t | n(t))/a(t)$, and hence the diffusion equation (9) in the co-moving coordinate system can be formulated as

$$\frac{\partial W(\mathbf{r}, t | n(t))}{\partial t} = \frac{D(n(t))}{a^2(t)} \nabla_{\mathbf{r}}^2 W(\mathbf{r}, t | n(t)), \quad (12)$$

the coefficient of which depends on the scale factor $a(t)$ since the Brownian motion is defined in physical space. Define the random functional

$$T(t) = \int_0^t \frac{D(n(t'))}{a^2(t')} dt'. \quad (13)$$

Then there exists $T'(t) = D(n(t))/a^2(t)$, so the diffusion equation (12) reduces to the standard diffusion equation for Brownian motion

$$\frac{\partial W(\mathbf{r}, T)}{\partial T} = \nabla_{\mathbf{r}}^2 W(\mathbf{r}, T). \quad (14)$$

Concerning the initial distribution of the CM, we employ the Dirac δ function in a non-static medium, i.e., $P(\bar{\mathbf{r}}, 0 | n_0) = \delta_{n, n_0} \delta(\bar{\mathbf{r}})$, and it is shown that $a(0) = 1$, $T(0) = 0$, implying

$W(\mathbf{r}, 0 | n_0) = \delta_{n, n_0} \delta(\mathbf{r})$. Under this initial condition, the solution of (14) via the scale transformation is a Gaussian function

$$W(\mathbf{r}, T) = \frac{e^{-\frac{\mathbf{r}^2}{4T}}}{(4\pi T)^{3/2}}. \quad (15)$$

To delineate the position of the CM, we utilize the subordinate method. In the co-moving coordinate system, the PDF of CM $W(\mathbf{r}, t | n_0)$ can be written as²⁹

$$W(\mathbf{r}, t | n_0) = \int_0^\infty \frac{e^{-\frac{\mathbf{r}^2}{4T}}}{(4\pi T)^{3/2}} P_T(T, t | n_0) dT, \quad (16)$$

in which $P_T(T, t | n_0)$ is the PDF of the subordinate process $T(t)$. From the definition of n -th order moment of the stochastic process, combining with (16) leads to

$$\begin{aligned} \langle \mathbf{r}^n(t) | n_0 \rangle &= \int_{R^3} \mathbf{r}^n W(\mathbf{r}, t | n_0) d\mathbf{r} \\ &= \int_0^\infty \int_{R^3} \mathbf{r}^n \frac{e^{-\frac{\mathbf{r}^2}{4T}}}{(4\pi T)^{3/2}} P_T(T, t | n_0) d\mathbf{r} dT. \end{aligned} \quad (17)$$

From (7), it is straightforward to obtain the n -th order moment in physical coordinate

$$\langle \bar{\mathbf{r}}^n(t) | n_0 \rangle = a^n(t) \langle \mathbf{r}^n(t) | n_0 \rangle. \quad (18)$$

Based on (17), the MSD in the co-moving coordinate system is

$$\langle \mathbf{r}^2(t) | n_0 \rangle = 6 \int_0^\infty T P_T(T, t | n_0) dT = 6 \langle T(t) | n_0 \rangle. \quad (19)$$

With regard to the first order moment of $T(t)$, from (13), one can get

$$\langle T(t) | n_0 \rangle = \int_0^t \sum_{n'=0}^\infty \frac{D_0}{a^2(t')(n' + n_{\min})^\beta} P_N(n', t' | n_0) dt'. \quad (20)$$

By taking the full expectation formula, it can be observed that $\langle T(t) \rangle = \langle \langle T(t) | n_0 \rangle \rangle$,

$$\langle T(t) \rangle = \int_0^t \sum_{n_0, n'} \frac{1}{a^2(t')} \frac{D_0}{(n' + n_{\min})^\beta} P_N(n', t' | n_0) P(n_0, 0) dt'. \quad (21)$$

Subsequently, it is necessary to calculate the statistics related to the CM, given that the initial size of the polymer conforms to the steady-state distribution $P(n_0, 0) \sim P^*(n_0)$. When $t \gg$

η , $P_N(n', t' | n_0) \sim P^*(n')$, the first order moment (21) reduces to

$$\begin{aligned} \langle T(t) \rangle &= \int_0^t \sum_{n_0, n'} \frac{1}{a^2(t)} \frac{D_0}{(n' + n_{\min})^\beta} P^*(n_0) P^*(n') dt' \\ &= D_0 \int_0^t \frac{1}{a^2(t')} dt' \langle (n + n_{\min})^{-\beta} \rangle, \end{aligned} \quad (22)$$

where $\sum_{n=0}^{\infty} \frac{D_0}{(n+n_{\min})^\beta} P^*(n) = D_0 \langle (n + n_{\min})^{-\beta} \rangle$. When $t \ll \eta$, $P_N(n', t' | n_0) \sim \delta_{n', n_0}$, $P(n_0, 0) \sim P^*(n_0)$, the first order moment of $T(t)$ is

$$\begin{aligned} \langle T(t) \rangle &= \int_0^t \sum_{n_0, n'} \frac{1}{a^2(t')} \frac{D_0}{(n' + n_{\min})^\beta} P^*(n_0) \delta_{n', n_0} dt' \\ &= D_0 \int_0^t \frac{1}{a^2(t')} dt' \langle (n + n_{\min})^{-\beta} \rangle. \end{aligned} \quad (23)$$

Within the physical coordinate system, the MSD for the CM in two scenarios $\langle \bar{r}^2(t) \rangle = a^2(t) \langle r^2(t) \rangle = 6a^2(t) \langle T(t) \rangle = 6a^2(t) \int_0^t \frac{1}{a^2(t')} dt' \langle (n + n_{\min})^{-\beta} \rangle$. Obviously, the MSD for the CM is contingent upon the size of the polymer and the non-static medium.

The statistics that characterizes the PDF of the stochastic process also encompasses the kurtosis K , which is principally utilized to quantify the tail of the PDF and describes the form of the PDF. In the physical coordinate \bar{x} direction of the non-static medium, we contemplate the property of the PDF for the CM of polymer, namely, the kurtosis in this direction is defined as^{42,43,50}.

$$K_{\bar{x}}(t) = \frac{\langle (\bar{x}(t) - \langle \bar{x}(t) \rangle)^4 \rangle}{\langle (\bar{x}(t) - \langle \bar{x}(t) \rangle)^2 \rangle^2}. \quad (24)$$

Different kurtosis values are associated with different PDF distributions, and kurtosis plays a significant role in quantifying non-Gaussian behavior, i.e., evaluating the deviation in the shape of the PDF from a Gaussian distribution. As a general rule, the kurtosis value 3 of the Gaussian distribution is selected as the standard, and compared with other cases, if $K > 3$, it is called leptokurtic, and if $K < 3$, it is called platykurtic. In this paper, the kurtosis is taken into account only in the physical coordinate system. Furthermore, exploiting the definition of kurtosis (24), here we sought to determine the expression for the fourth order moment $\langle (\bar{x}(t) - \langle \bar{x}(t) \rangle)^4 \rangle$. From the previous expressions (17) and (18), it can be indicated that in the direction of \bar{x} there is $\langle \bar{x}(t) \rangle = 0$. Consequently, the expression for kurtosis can be simplified as

$$K_{\bar{x}}(t) = \frac{\langle \bar{x}^4(t) \rangle}{\langle \bar{x}^2(t) \rangle^2}. \quad (25)$$

Analogously, the fourth order moment $\langle x(t)^4 \rangle = 12 \langle T^2(t) \rangle$ is first got in the co-moving coordinate system when the initial conditions satisfy the steady state distribution. Concerning $\langle T^2(t) \rangle$, once again combining the definition of $T(t)$ and the

equation of full expectation, there exists

$$\begin{aligned} \langle T^2(t) \rangle &= \int_0^t \int_0^t \sum_{n_0, n', n''} \frac{D_0}{a^2(t') (n' + n_{\min})^\beta} \frac{D_0}{a^2(t'') (n'' + n_{\min})^\beta} P(n_0, 0) \\ &\quad \times P_N(n'', t'', n', t' | n_0) dt' dt'' \\ &= \int_0^t \int_0^t \sum_{n_0, n', n''} \frac{D_0}{a^2(t') (n' + n_{\min})^\beta} \frac{D_0}{a^2(t'') (n'' + n_{\min})^\beta} P(n_0, 0) \\ &\quad \times P_N(n'', t'' | n', t', n_0) P_N(n', t' | n_0) dt' dt'' \\ &= \int_0^t \int_0^t \sum_{n_0, n', n''} \frac{D_0}{a^2(t') (n' + n_{\min})^\beta} \frac{D_0}{a^2(t'') (n'' + n_{\min})^\beta} P(n_0, 0) \\ &\quad \times P_N(n'', t'' | n', t') P_N(n', t' | n_0) dt' dt''. \end{aligned} \quad (26)$$

The conditional probability property of three events is utilized in the progression from the first equal sign to the second equal sign $P_N(n'', t'', n', t' | n_0) = P_N(n', t' | n_0) P_N(n'', t'' | n', t', n_0)$. In the transition from the second equals sign to the third equals sign, the Markov property of Markov processes is utilized, indicating that the present state is exclusively related to the state of the preceding moment and is irrelevant to the previous state, so $P_N(n'', t'' | n', t', n_0) = P_N(n'', t'' | n', t')$. When $t', t'' \gg \eta$ and $t'' - t' \gg \eta$, due to the time homogeneous of the birth and death process, there exists $P_N(n'', t'' | n', t') = P_N(n'', t'' - t' | n', 0) \sim P^*(n'')$; in this case the second order moment of $T(t)$ is

$$\begin{aligned} \langle T^2(t) \rangle &= \int_0^t \int_0^t \sum_{n_0, n', n''} \frac{D_0}{a^2(t') (n' + n_{\min})^\beta} \frac{D_0}{a^2(t'') (n'' + n_{\min})^\beta} \\ &\quad \times P^*(n_0) P^*(n') P^*(n'') dt' dt'' \\ &= \left(D_0 \int_0^t \frac{1}{a^2(t')} dt' \langle (n + n_{\min})^{-\beta} \rangle \right)^2. \end{aligned} \quad (27)$$

Similarly, $\langle T^2(t) \rangle = \left(D_0 \int_0^t \frac{1}{a^2(t')} dt' \right)^2 \langle (n + n_{\min})^{-2\beta} \rangle$, as $t', t'' \ll \eta$. By converting the MSD and fourth order moment in the co-moving coordinate system to the physical coordinate system, the kurtosis in the physical coordinate system can be obtained

$$\begin{aligned} K_{\bar{x}} &= \frac{\langle \bar{x}^4(t) \rangle}{\langle \bar{x}^2(t) \rangle^2} = \frac{a^4(t) \langle x^4(t) \rangle}{(a^2(t) \langle x^2(t) \rangle)^2} \\ &= 3 \frac{a^4(t) \langle T^2(t) \rangle}{(a^2(t) \langle T(t) \rangle)^2} \sim \begin{cases} 3 \frac{\langle (n+n_{\min})^{-2\beta} \rangle}{\langle (n+n_{\min})^{-\beta} \rangle^2} & t \ll \eta, \\ 3 & t \gg \eta. \end{cases} \end{aligned} \quad (28)$$

In short time, the PDF for the CM shows a non-Gaussian distribution, but in long time limit, the PDF tends to a Gaussian distribution. With the distribution of the stochastic process $T(t)$, the Gaussian mixed PDF for the CM has a fat-tail feature from (16). Nevertheless, the PDF returns to a Gaussian distribution when the stochastic process $T(t)$ tends to be steady state.

A. Power-law scale factor

Power-law media have widespread applications in nature and engineering, such as fluid transport through porous media in geology and market fluctuations in finance. Investigating the diffusion behavior of power-law media is essential to interpret physical and chemical phenomena. With homogeneous media, the time evolution of a power-law medium is stated by a power-law form^{17,18}

$$a(t) = \left(\frac{t+t_0}{t_0} \right)^\gamma. \quad (29)$$

The value of the index γ reflects different media types, $\gamma > 0$ means that the media type is expanding, $\gamma < 0$ corresponds to contracting media, and $\gamma = 0$ represents that the media is static. Power-law exponent has many arduous types of applications in cosmology, in simpler terms, when $\gamma = 1/2$, radiation dominates the universe's expansion; when $\gamma = 2/3$, matter does. Next, we should pay attention to the MSD in the direction of \bar{x} for the CM via (19) and (22), we start by calculating

$$\begin{aligned} \int_0^t \frac{1}{a^2(t')} dt' &= \int_0^t \left(\frac{t'+t_0}{t_0} \right)^{-2\gamma} dt' \\ &= \begin{cases} \frac{t_0}{2\gamma-1} \left(1 - \left(\frac{t+t_0}{t_0} \right)^{1-2\gamma} \right) & \gamma \neq \frac{1}{2}, \\ t_0 \ln \left(\frac{t+t_0}{t_0} \right) & \gamma = \frac{1}{2}. \end{cases} \end{aligned} \quad (30)$$

In the long-time limit $t \rightarrow \infty$, using the above equation (30) to classify the power-law medium by using $1/2$ as the critical value of γ , the asymptotic behavior of the MSD in the co-moving coordinate system can be categorically represented as

$$\begin{aligned} \langle \bar{x}^2(t) \rangle &= 2\langle T(t) \rangle \\ &\sim \begin{cases} \frac{2t_0}{2\gamma-1} D_0 \langle (n+n_{\min})^{-\beta} \rangle & \gamma > \frac{1}{2}, \\ 2t_0 \ln \left(\frac{t+t_0}{t_0} \right) D_0 \langle (n+n_{\min})^{-\beta} \rangle & \gamma = \frac{1}{2}, \\ \frac{2t_0^{2\gamma} t^{1-2\gamma}}{1-2\gamma} D_0 \langle (n+n_{\min})^{-\beta} \rangle & \gamma < \frac{1}{2}. \end{cases} \end{aligned} \quad (31)$$

In co-moving coordinate system, while $\gamma > 1/2$, the MSD for the CM tends to stabilize after a sufficiently long time and asymptotes to a constant related to the mean of birth and death process and power law exponent. As is apparent, if the medium expands rapidly, i.e., in a strong expanding media, the movement of the polymer is dominated by the expanding media and the diffusion of the polymer itself is negligible. When media expansion is controlled by radiation $\gamma = 1/2$, the MSD increases logarithmically. In case $\gamma < 1/2$, the MSD grows with time as power law with the order of $1-2\gamma$.

The long time asymptotic expression of the MSD in the physical coordinate system can be directly obtained from the relation (18) as

$$\begin{aligned} \langle \bar{x}^2(t) \rangle &= a^2(t) \langle \bar{x}^2(t) \rangle \\ &\sim \begin{cases} \frac{2t_0^{1-2\gamma} t^{2\gamma}}{2\gamma-1} D_0 \langle (n+n_{\min})^{-\beta} \rangle & \gamma > \frac{1}{2}, \\ 2t \ln \left(\frac{t+t_0}{t_0} \right) D_0 \langle (n+n_{\min})^{-\beta} \rangle & \gamma = \frac{1}{2}, \\ \frac{2t}{1-2\gamma} D_0 \langle (n+n_{\min})^{-\beta} \rangle & \gamma < \frac{1}{2}. \end{cases} \end{aligned} \quad (32)$$

In physical coordinate system, the CM asymptotically exhibits superdiffusion after a sufficiently long time as $\gamma > 1/2$. The motion for the CM in relatively strong expanding media depends mainly on the expansion of the medium, which is reinforced by the results in co-moving coordinate system. For $\gamma < 1/2$, the CM asymptotically exhibits normal diffusion in weakly expanding or contracting media, where the intrinsic Brownian motion of the polymer plays a dominant role. The simulation results are shown in Fig 1. There are similar conclusions for Brownian motion and the motion with waiting time obeying exponential distribution in non-static media.

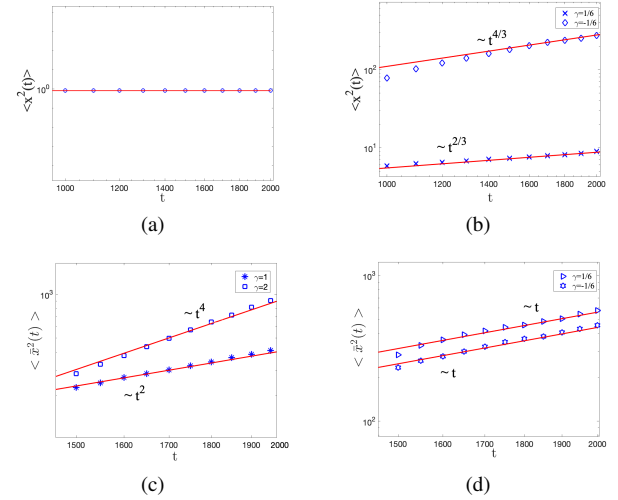


FIG. 1. Numerical simulations of the MSD for the CM in a power-law medium. The red solid lines in the figure represent our theoretical results (31) and (32). The parameters related to the random diffusion coefficient are $D_0 = 1$, $n_{\min} = 3$, $\lambda = 0.45$, $\mu = 0.5$, $\beta = 1$, and the initial values $x_0 = 1$ and $\bar{x}_0 = 1$. The simulation results are emphasized in blue, where $\gamma = 1$ in Fig. (a), and $\gamma = -1/6$ (diamond), $\gamma = 1/6$ (cross) in Fig. (b); ballistic diffusion for $\gamma = 1$ (asterisk), $\gamma = 2$ (square) in Fig. (c), and for Fig. (d) $\gamma = -1/6$ (hexagon), $\gamma = 1/6$ (triangle).

B. Exponential scale factor

The exponential media shows an exponential distribution on the time scale. It has extensive applications in the fields of geophysics, financial engineering, and biomedicine, such as surveying earthquakes, describing the spatial and temporal evolution of stock prices and interest rates, and studying the dynamics of proteins inside cells. The exponential media is defined by the exponential scale factor^{17,18}, as follows

$$a(t) = e^{Ht}. \quad (33)$$

The H is the Hubble parameter, defined as $a'(t)/a(t)$. In cosmology, the exponential scaling factor describes that the expansion of the universe is dominated by dark energy, $H > 0$ corresponds to the exponentially expanding media, $H < 0$ corresponds to the exponentially contracting media, and $H = 0$ is for the static media that we previously default to in this study.

In the same way, let us take into consideration of the MSD in the \bar{x} direction of the exponential medium after a long time. The MSD for the CM in the co-moving coordinate system behaves as

$$\langle x^2(t) \rangle = 2\langle T(t) \rangle \sim \begin{cases} \frac{1}{H} D_0 \langle (n + n_{\min})^{-\beta} \rangle & H > 0, \\ \frac{(e^{2|H|t} - 1)}{|H|} D_0 \langle (n + n_{\min})^{-\beta} \rangle & H < 0. \end{cases} \quad (34)$$

For $H > 0$, the MSD in the co-moving coordinate system tends to be a constant regarding the Hubble parameter and the mean value of birth and death process for sufficiently long time, whereas it increases exponentially in the contracting media $H < 0$.

In the physical coordinate system, the asymptotic expression for the MSD turns out to be

$$\langle \bar{x}^2(t) \rangle = a^2(t) \langle x^2(t) \rangle \sim \begin{cases} \frac{(e^{2Ht} - 1)}{H} D_0 \langle (n + n_{\min})^{-\beta} \rangle & H > 0, \\ \frac{1}{|H|} D_0 \langle (n + n_{\min})^{-\beta} \rangle & H < 0. \end{cases} \quad (35)$$

For $H > 0$, the MSD for the CM in the physical coordinate system proceeds exponentially with time t . However, for $H < 0$, the MSD for the CM asymptotes to a constant in a time long enough. It can be observed that the motion of the polymer in the exponential medium is dominated by the medium and the intrinsic Brownian motion is ignored, which is a situation similar to the motion of the polymer in a power-law strongly expanding media. Simulation results of MSD in exponential medium in co-moving and physical coordinates are shown in Fig 2. Additionally, the odd order moments for the CM can be revealed to be zero by (17) and (18).

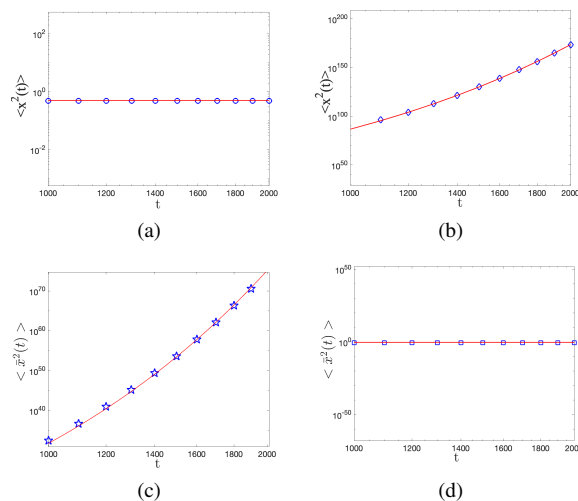


FIG. 2. Numerical simulations of the MSD for the CM in the exponential medium. In Figs. (a) and (c), $H = 0.1$, and in Figs. (b) and (d), $H = -0.1$; the red solid lines represent the theoretical results (34) and (35), and the blue marks indicate the simulation results.

IV. BIVARIATE FOKKER-PLANCK EQUATION AND FEYNMAN-KAC EQUATION

In the first part of this section, we adopt a subordinate approach and combine the Feynman-Kac equation for the birth and death process to obtain the bivariate Fokker-Planck equation satisfied by the PDF for the CM in the physical coordinate system. The second part focuses on the DD model in 1-dimensional space, and the Feynman-Kac equation corresponding to the DD model defined by the overdamped Langevin equation is derived.

A. Derivation of the bivariate Fokker-Planck equation

Fokker-Planck equation describes the evolution of the PDF of the position for a stochastic process with time. On the basis of the non-static extension for the polymer CM motion in Section III, noticeably, the position of the CM rests on the size of the polymer, furthermore on the Brownian motion of the polymer as a whole. Primarily, we avail ourselves of the subordinate process approach to derive the bivariate Fokker-Planck equations corresponding to the DD model in Section III.

Utilizing the subordination expression, the PDF of the bivariate in the co-moving coordinate system behaves as

$$g(\mathbf{r}, n, t) = \int_0^\infty W(\mathbf{r}, T) O(n, T, t) dT, \quad (36)$$

the left hand side of which $g(\mathbf{r}, n, t)$ denotes the probability of the number of monomers n and the CM position \mathbf{r} at the moment t in the co-moving coordinate system. On the right side of the equal sign, the first term $W(\mathbf{r}, T)$ represents the Gaussian PDF, which satisfies $\frac{\partial}{\partial T} W(\mathbf{r}, T) = \nabla_{\mathbf{r}}^2 W(\mathbf{r}, T)$. The second term $O(n, T, t)$ is the joint PDF of the number of monomers n and the functional T at t moment. From the definition of $T(t)$, it follows that $T(t)$ is a functional of the birth and death process $n(t)$ and the non-static media $a(t)$. Based on the Appendix A, the Feynman-Kac equation that $O(n, T, t)$ satisfies is

$$\frac{\partial O(n, T, t)}{\partial t} = \Phi_n O(n, T, t) - \frac{D(n)}{a^2(t)} \frac{\partial}{\partial T} O(n, T, t). \quad (37)$$

Let us capitalize (36), incorporating (37) and (14) in the previous section, to derive bivariate Fokker-Planck equation in the co-moving coordinate system

$$\begin{aligned} & \frac{\partial g(\mathbf{r}, n, t)}{\partial t} \\ &= \int_0^\infty W(\mathbf{r}, T) \frac{\partial O(n, T, t)}{\partial t} dT \\ &= \int_0^\infty W(\mathbf{r}, T) \left(\Phi_n O(n, T, t) - \frac{D(n)}{a^2(t)} \frac{\partial O(n, T, t)}{\partial T} \right) dT \quad (38) \\ &= \Phi_n g(\mathbf{r}, n, t) + \frac{D(n)}{a^2(t)} \int_0^\infty O(n, T, t) \nabla_{\mathbf{r}}^2 W(\mathbf{r}, T) dT \\ &= \Phi_n g(\mathbf{r}, n, t) + \frac{D(n)}{a^2(t)} \nabla_{\mathbf{r}}^2 g(\mathbf{r}, n, t), \end{aligned}$$

where Φ_n is defined in (A5). Let $p(\bar{\mathbf{r}}, n, t)$ be the corresponding PDF of $g(\mathbf{r}, n, t)$ in the physical coordinate system. By exploiting the relationship between the PDFs of two coordinates and harnessing the method in the literature⁴ once again, contrary to the previous one, on this occasion the PDF in the co-moving coordinate system is switched to the physical coordinate system, and it is possible to derive the bivariate Fokker-Planck equation satisfied by the PDF $p(\bar{\mathbf{r}}, n, t)$, i.e.,

$$\frac{\partial p(\bar{\mathbf{r}}, n, t)}{\partial t} = -\frac{d'(t)}{a(t)} \nabla_{\bar{\mathbf{r}}} \cdot (\bar{\mathbf{r}} p(\bar{\mathbf{r}}, n, t)) + \Phi_n p(\bar{\mathbf{r}}, n, t) + D(n) \nabla_{\bar{\mathbf{r}}}^2 p(\bar{\mathbf{r}}, n, t). \quad (39)$$

B. Derivation of the Feynman-Kac equation

The researchers propose a DD model⁵¹ using the overdamped Langevin equation to describe a Brownian non-Gaussian process, where the diffusion coefficient $D(t)$ is a stochastic function relevant to the Ornstein-Uhlenbeck process. Literature¹³ investigates the DD model for scaled Brownian motion along with the simulation for the PDF of the particles in a long time. Two DD models with external forces⁵² are studied, and the difference among these two models is whether or not they satisfy the fluctuation-dissipation theorem, and the diffusion equations are deduced, respectively. For the sake of convenience, we concentrate on the Feynman-Kac equation of the DD model in the 1-dimensional case

$$d\bar{x}(t) = \frac{d'(t)}{a(t)} \bar{x}(t) dt + \sqrt{2D(n(t))} dB(t). \quad (40)$$

Define the functional of $\bar{x}(t)$ as

$$A_2 = \int_0^t U(\bar{x}(t')) dt', \quad (41)$$

where $\bar{x}(t)$ represents the path of the stochastic process, the diffusion coefficient $D(n(t))$ is a stochastic function with respect to the birth death process, and $U(\bar{x}(t))$ should be specified in the context of the practical problem. By taking particular U , one can determine the distribution of the occupation time of the particle, distribution of the first passage times, and the area under the path curve⁵³, etc. To derive specifically the Feynman-Kac equation relative to DD model, firstly the increment of CM displacement in the \bar{x} direction together with the functional A_2 in the $(t, t + \tau)$ time period are concerned,

respectively,

$$\bar{x}(t + \tau) - \bar{x}(t) \simeq \frac{d'(t)}{a(t)} \bar{x}(t) \tau + \sqrt{2D(n(t))} (B(t + \tau) - B(t)) \quad (42)$$

and

$$A_2(t + \tau) - A_2(t) = \int_t^{t+\tau} U(\bar{x}(t')) dt' \simeq U(\bar{x}(t)) \tau. \quad (43)$$

With respect to the CM displacement and functional A_2 increments, we resort to the Itô integral, i.e., the integrand function takes the value of the left endpoint of the interval. Consequently, $\bar{x}(t)$ and $D(n(t))$ are both independent of the increments of $B(t)$ over the time period $(t, t + \tau)$. The increment $(B(t + \tau) - B(t))$ is a stationary random process and has the same distribution as $B(\tau)$, i.e., it obeys a normal distribution with 0 mean and variance τ , and its characteristic function is

$$\left\langle e^{-ik(B(t+\tau)-B(t))} \right\rangle = e^{-\frac{k^2\tau}{2}}. \quad (44)$$

Moreover, in conjunction with our discussion of the birth and death process in Section II, the increment can be written in the form

$$f(n(t + \tau)) - f(n(t)) \simeq \lambda \tau f(n(t) + 1) + \mu \tau f(n(t) - 1) - (\mu + \lambda) \tau f(n(t)). \quad (45)$$

Denoting the joint PDF for the CM position \bar{x} , the number of monomers n , and the functional A_2 at moment t by $G(\bar{x}, n, A_2, t)$, then

$$G(\bar{x}, n, A_2, t) = \langle \delta(\bar{x} - \bar{x}(t)) \delta(A_2 - A_2(t)) \delta_{n, n(t)} \rangle. \quad (46)$$

Predominantly deriving the Feynman-Kac equation in Fourier space, the Fourier transform of the joint PDF $G(\bar{x}, n, A_2, t)$ is

$$G(k, l, p_2, t) = \sum_n \int_{-\infty}^{\infty} \int_{-\infty}^{\infty} e^{-ik\bar{x} - ip_2 A_2 - iln} G(\bar{x}, n, A_2, t) d\bar{x} dA_2 = \left\langle e^{-ik\bar{x}(t)} e^{-iln(t)} e^{-ip_2 A_2(t)} \right\rangle, \quad (47)$$

in which the variables relative to the time domain space and the Fourier space are $\bar{x} \rightarrow k$, $n \rightarrow l$, and $A_2 \rightarrow p_2$, respectively. The increment of the joint PDF $G(\bar{x}, n, A_2, t)$ in Fourier space is

$$G(k, l, p_2, t + \tau) - G(k, l, p_2, t) = \left\langle e^{-ik\bar{x}(t+\tau)} e^{-iln(t+\tau)} e^{-ip_2 A_2(t+\tau)} \right\rangle - \left\langle e^{-ik\bar{x}(t)} e^{-iln(t)} e^{-ip_2 A_2(t)} \right\rangle. \quad (48)$$

Substituting the CM displacement increment (42), the functional increment (43), and the increment of birth death process (45) into (48), there exists

$$\begin{aligned}
 & G(k, l, p_2, t + \tau) - G(k, l, p_2, t) \\
 & \simeq \left\langle e^{-ik\bar{x}(t)} e^{-iln(t)} e^{-ip_2 A_2(t)} \left((1 + \lambda \tau e^{-il} + \mu \tau e^{il} - (\mu + \lambda) \tau) e^{-ik \left(\frac{d'(t)}{a(t)} \bar{x}(t) \tau + \sqrt{2D(n(t))} (B(t+\tau) - B(t)) \right)} e^{-ip_2 U(\bar{x}(t)) \tau} - 1 \right) \right\rangle \quad (49) \\
 & \simeq \left\langle e^{-ik\bar{x}(t)} e^{-iln(t)} e^{-ip_2 A_2(t)} \left(\left(-ik \frac{d'(t)}{a(t)} \bar{x}(t) \tau - D(n(t)) k^2 \tau - ip_2 U(\bar{x}(t)) \tau \right) + (\lambda \tau e^{-il} + \mu \tau e^{il} - (\mu + \lambda) \tau) \right) \right\rangle,
 \end{aligned}$$

in which the Taylor expansion is deployed to ignore higher order terms, and the mutual independence of $D(n(t))$ and the

increment of Brownian motion is also used. Dividing both sides of (49) by τ , and taking the limit $\tau \rightarrow 0$, we obtain

$$\begin{aligned}
 & \frac{\partial}{\partial t} G(k, l, p_2, t) \\
 & = -ik \left\langle e^{-ik\bar{x}(t)} e^{-iln(t)} e^{-ip_2 A_2(t)} \frac{d'(t)}{a(t)} \bar{x}(t) \right\rangle - k^2 \left\langle e^{-ik\bar{x}(t)} e^{-iln(t)} e^{-ip_2 A_2(t)} D(n(t)) \right\rangle - ip_2 \left\langle e^{-ik\bar{x}(t)} e^{-iln(t)} e^{-ip_2 A_2(t)} U(\bar{x}(t)) \right\rangle \\
 & + \left\langle \lambda e^{-ik\bar{x}(t)} e^{-il(n(t)+1)} e^{-ip_2 A_2(t)} + \mu e^{-ik\bar{x}(t)} e^{-il(n(t)-1)} e^{-ip_2 A_2(t)} - (\mu + \lambda) e^{-ik\bar{x}(t)} e^{-iln(t)} e^{-ip_2 A_2(t)} \right\rangle. \quad (50)
 \end{aligned}$$

Capitalizing on the time-shift property of the Fourier transform $\mathcal{F}_{n \rightarrow l} \{f(n \pm c)\} = e^{\pm ilc} f(k)$ and the derivative prop-

erty, after performing an inverse Fourier transform on both sides of (50), the Feynman-Kac equation for the joint PDF $G(\bar{x}, n, A_2, t)$ can be organized as follows

$$\frac{\partial G(\bar{x}, n, A_2, t)}{\partial t} = -\frac{d'(t)}{a(t)} \frac{\partial}{\partial \bar{x}} (\bar{x} G(\bar{x}, n, A_2, t)) + D(n) \frac{\partial^2}{\partial \bar{x}^2} G(\bar{x}, n, A_2, t) + \Phi_n G(\bar{x}, n, A_2, t) - U(\bar{x}) \frac{\partial}{\partial A_2} G(\bar{x}, n, A_2, t). \quad (51)$$

V. SIMULATIONS

In this section, we present the simulation results by solving our derived Fokker-Planck equation and Feynman-Kac equation, by using the deep BSDE method and the Monte Carlo method, respectively. The initial value problem must be first transformed into a terminal problem through the time transformation $t \rightarrow T - t$. All numerical examples are executed on a desktop computer with a 3.40GHz Intel Core i7 processor and 32 GB of memory.

A. Joint Distribution of CM Positions

In this subsection, we examine the joint probability distribution of the polymer size and the position of the CM, with consideration of the forward Fokker-Planck equation

$$\begin{aligned}
 & \frac{\partial}{\partial t} p(\bar{r}, n, t) - \frac{d'(T-t)}{a(T-t)} \nabla_{\bar{r}} \cdot (\bar{r} p(\bar{r}, n, t)) \\
 & + \Phi_n p(\bar{r}, n, t) + D(n) \nabla_{\bar{r}}^2 p(\bar{r}, n, t) = 0, \quad (52)
 \end{aligned}$$

the terminal condition of which is $p(\bar{r}, n, T) = g(\bar{r}, n)$.

Let us consider the following parameters: $d = 2$, $D_0 = 2$, $n_{\min} = 3$, $\beta = 1$, $T = 0.5$, $\beta(n) = \lambda = 2$, $\alpha(n) = \mu =$

1, $a(t) = e^t$. Additionally, we assume that the terminal condition is given by

$$g(\bar{r}, n) = \frac{\mathcal{K}_{\{0, \dots, 9\}}(n)}{10(2\pi)^{\frac{1}{2}}} e^{-\frac{|\bar{r}|^2}{2}}. \quad (53)$$

We plot the results of deep BSDE method and its relative error relative to the ‘‘exact solution’’ obtained by Monte Carlo simulation (Fig. 3). The results of the deep BSDE method go through 80,000 iterations with a batch size of 2048 at 40 equidistant time steps ($N = 40$), with a learning rate of 0.0004 for the first 40,000 iterations and 0.0001 for the last 40,000 iterations. The results demonstrate that the solution obtained by solving (52) is consistent with the solution obtained through Monte Carlo simulation.

B. Joint Distribution of Position Integral Functional

This subsection explores and discusses the joint probability distribution of size, position, and position-integral functions for polymer CM. The functional relevant to this application is

$$A_2 = \int_0^t |\bar{x}(t')|^2 dt'. \quad (54)$$

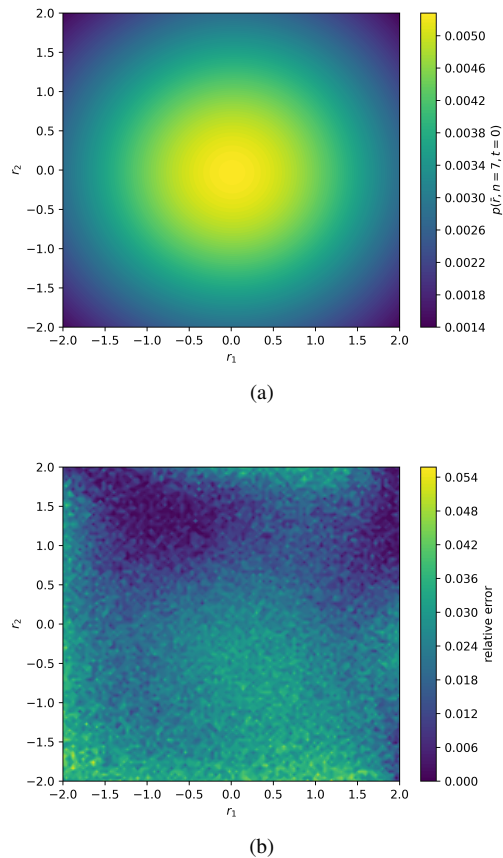


FIG. 3. (a) Plot of $\phi(x|\theta_\phi)$ as an approximation of $p(\bar{x}, n = 7, t = 0)$ for the deep BSDE method. (b) Relative error of the deep BSDE method for $p(\bar{x}, n = 7, t = 0)$, where the “exact solution” is obtained by the Monte Carlo method.

By respectively employing the deep BSDE method and Monte Carlo simulation to solve the forward Feynman-Kac equation

$$\begin{aligned}
 \frac{\partial}{\partial t} \tilde{G}(\bar{x}, n, p, t) - \frac{a'(T-t)}{a(T-t)} \nabla_{\bar{x}} \cdot (\bar{x} \tilde{G}(\bar{x}, n, p, t)) + \Phi_n \tilde{G}(\bar{x}, n, p, t) \\
 + \frac{D_0}{(n+n_{\min})^\beta} \nabla_{\bar{x}}^2 \tilde{G}(\bar{x}, n, p, t) - ip|\bar{x}|^2 \tilde{G}(\bar{x}, n, p, t) = 0,
 \end{aligned} \quad (55)$$

with terminal condition $\tilde{G}(\bar{x}, n, p, T) = g(\bar{x}, n, p)$, we get the joint probability distribution.

Considering the following parameters: $d = 2, D_0 = 2, n_{\min} = 3, \beta = 0.5, n = 4, \bar{x} = 0, T = 0.5, \beta(n) = \lambda = 2, \lambda(n) = \mu = 1.5, a(t) = \frac{t+0.5}{0.5}$, and the terminal condition

$$g(\bar{x}, n, p) = \frac{\kappa_{\{0, \dots, 4\}}(n)}{5(2\pi)^{\frac{1}{2}}} e^{-\frac{|\bar{x}|^2}{2}}, \quad (56)$$

we acquire the results of the two methods (Fig. 4). We divide $p \in [-75, 75]$ into five parts on average, and train five deep BSDE models in parallel, where each model goes through 200,000 iterations of 1024 batch size at 50 equidistant time steps ($N = 50$), with a learning rate of 0.0004 for the first

100,000 and 0.0001 for the last 100,000 iterations. The final results can then be obtained by inverse Fourier transform. The L_2 relative error between the solution obtained by the deep BSDE method and the solution obtained by the Monte Carlo simulation reaches 0.0757. The results indicate that the solution obtained by solving (55) is consistent with the solution obtained by Monte Carlo simulation.

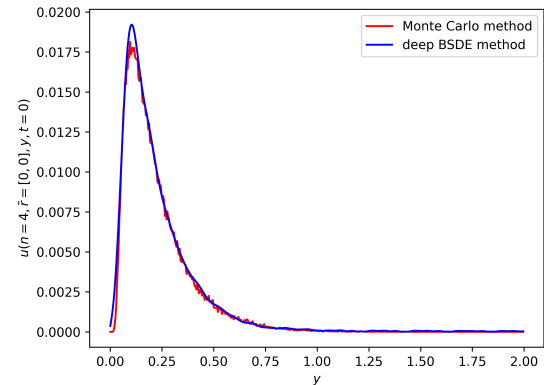


FIG. 4. Probability density of first passage time of polymer CM at $n = 4, \bar{x} = [0, 0], t = 0$, and $A_2 \in [0, 2]$, which are obtained by deep BSDE method and Monte Carlo simulation, respectively. The red line represents the “exact solution” obtained by Monte Carlo simulation, and the blue line is for the solution obtained by solving (55) using deep BSDE method and making inverse Fourier transform.

VI. CONCLUSION

We establish a DD model by describing the polymerization and depolymerization of the polymer, and introducing the co-moving and physical coordinate to characterize the dynamic behavior in the non-static medium. We also discuss in different media what dominates the CM motion. More deeply, we study the bivariate Fokker-Planck and Feynman-Kac equations corresponding to the DD model. Firstly, according to the subordinate equation, we obtain the diffusion equation satisfied by the bivariate PDF of the CM in the co-moving coordinate system, and then make a transformation to the physical coordinate system by utilizing the relation between the two coordinates. It is worth noting that we also focus on the diffusion-diffusion model in the sense of Itô, and combine with the properties of the Fourier transform to derive the Feynman-Kac equation of the joint PDF $G(\bar{x}, n, A_2, t)$. In addition, we solve the corresponding Fokker-Planck and Feynman-Kac equations for the DD model using deep BSDE method and verify their plausibility through simulations with the Monte Carlo method.

In this paper, we have found that the Brownian non-Gaussian diffusion behavior of the CM of polymer is related to the variation of the polymer size and the expansion/contraction of the media. The following questions can be further explored in a non-static medium as the next step: 1. Investigate the CM dynamical behavior, where the chemical

reaction rates depend on the number of polymer monomers in a limited-polymer-monomer environment; 2. Study the overall Brownian motion of the polymer, the effects of the polymer's own depolymerization and polymerization, and the random changes in time on the position of the CM.

DATA AVAILABILITY STATEMENT

The data that support the findings of this study are available on request from the corresponding author.

Appendix A: Derivation of (37)

The Feynman-Kac equation is universally resorted for characterizing the PDF fulfilled by the particle generalized distribution, and next our objective is to obtain the Feynman-Kac equation in which the joint PDF $O(n, A, t)$ resides. The functional of $n(t)$ is defined as

$$A_1 = \int_0^t U(n(t'), t') dt', \quad (A1)$$

where the function $U(n, t)$ depends not only on $n(t)$ but also explicitly on time. The functional $T(t) = \int_0^t \frac{D(n(t'))}{a^2(t')} dt'$ in the present research is specific.

For not losing generality, in the following discussion we use the functional A_1 . In accordance with the discussion of the birth and death process in Section II, the process of birth and death can be viewed as a continuous random time walk, i.e., no reaction occurs at $(t, t + \tau)$, and after waiting for time τ , the depolymerization or polymerization of monomers occurs at the $t + \tau$ moment. As a result, the $t + \tau$ of the functional is linked to the t moment as follows

$$\begin{aligned} A_1(t + \tau) &= \int_0^{t+\tau} U(n(t'), t') dt' \\ &= \int_0^t U(n(t'), t') dt' + \int_t^{t+\tau} U(n(t), t') dt' \quad (A2) \\ &= A_1(t) + \int_t^{t+\tau} U(n(t), t') dt'. \end{aligned}$$

Represent the joint PDF for the number of monomers n and the functional A_1 at $t + \tau$ moment by $O(n, A_1, t + \tau)$. From the master equation (4) and the relation (A2) in Section II, in the

case of $n \geq 1$, it can be obtained

$$\begin{aligned} &O(n, A_1, t + \tau) \\ &= \mu \tau O(n + 1, A_1 - \int_t^{t+\tau} U(n + 1, t') dt', t) \\ &\quad + \lambda \tau O(n - 1, A_1 - \int_t^{t+\tau} U(n - 1, t') dt', t) \\ &\quad + (1 - \mu \tau - \lambda \tau) O(n, A_1 - \int_t^{t+\tau} U(n, t') dt', t). \end{aligned} \quad (A3)$$

Making the Fourier transform $A_1 \rightarrow p_1$ on both sides of (A3) and combining the time shift property of Fourier transform $\mathcal{F}_{A_1 \rightarrow p_1} \{f(A_1 - c)\} = e^{-ip_1 c} f(p_1)$ result in

$$\begin{aligned} &O(n, p_1, t + \tau) \\ &= \mu \tau e^{-ip_1 \int_t^{t+\tau} U(n+1, t') dt'} O(n + 1, p_1, t) \\ &\quad + \lambda \tau e^{-ip_1 \int_t^{t+\tau} U(n-1, t') dt'} O(n - 1, p_1, t) \\ &\quad + (1 - \mu \tau - \lambda \tau) e^{-ip_1 \int_t^{t+\tau} U(n, t') dt'} O(n, p_1, t). \end{aligned} \quad (A4)$$

After dividing (A4) by τ , letting $\tau \rightarrow 0$, and ignoring the high-order terms, then one can get

$$\frac{\partial O(n, p_1, t)}{\partial t} = \Phi_n O(n, p_1, t) - ip_1 U(n, t) O(n, p_1, t), \quad (A5)$$

where the operator Φ_n is defined as $\Phi_n O(n) = \mu O(n + 1) + \lambda O(n - 1) - (\mu + \lambda) O(n)$. Taking inverse Fourier transform simultaneously on both sides of (A5) leads to

$$\frac{\partial O(n, A_1, t)}{\partial t} = \Phi_n O(n, A_1, t) - U(n, t) \frac{\partial}{\partial A_1} O(n, A_1, t), \quad (A6)$$

in which

$$\mathcal{F}_{A_1} \left\{ -\frac{\partial}{\partial A_1} U(n, t) O(n, A_1, t) \right\} = -ip_1 U(n, t) O(n, p_1, t).$$

Appendix B: Deep BSDE Method

The deep BSDE method, as presented in a recently published paper⁵⁴, represents a class of deep learning methods designed for solving high-dimensional partial differential equations (PDEs). Subsequently, a discrete version of the BSDE method is developed, and it is successfully used to solve the PDEs with infinite dimensional discrete operators⁵⁵. For the convenience of readers, this part will provide a brief introduction of the fundamental concepts underlying the deep BSDE method, and make it adapted to the PDEs considered in this paper.

1. PDEs and BSDEs

Our investigation primarily focuses on a class of semilinear parabolic PDEs with infinite dimensional discrete operator. These PDEs can be uniformly represented as the form

$$\frac{\partial}{\partial t} u(x, n, p, t) - \frac{d'(T-t)}{a(T-t)} \nabla_x \cdot (xu(x, n, p, t)) + T_n u(x, n, p, t) + \frac{D_0}{(n+n_{\min})^\beta} \nabla_x^2 u(x, n, p, t) + f(x, n, p, u(x, n, p, t)) = 0, \quad (\text{B1})$$

the terminal condition of which is $u(x, n, p, T) = g(x, n, p)$, and the unknown is $u : \mathbb{N} \times \mathbb{R}^d \times \mathbb{R}^1 \times [0, T) \rightarrow \mathbb{C}$,

$$T_n f(n) = \begin{cases} \alpha(n)(f(n+1) - f(n)) + \beta(n)(f(n-1) - f(n)), & n \geq 1, \\ \alpha(n)(f(1) - f(0)), & n = 0, \end{cases} \quad (\text{B2})$$

where $\alpha(n)$ and $\beta(n)$ are given functions satisfying $\alpha(n), \beta(n) \geq 0$ for $n \in \mathbb{N}$, and $\beta(0) = 0$. Obviously, Eqs. (39)

and (51) can both be changed as the form of (B1). Let $n(t)$ be a birth and death process satisfying

$$\mathbb{P}(n(t+\tau) - n(t) = k | n(t) = n) = \begin{cases} \alpha(n)\tau + o(\tau), & k = 1, \\ \beta(n)\tau + o(\tau), & k = -1, \\ 1 - (\alpha(n) + \beta(n))\tau + o(\tau), & k = 0, \\ o(\tau), & \text{otherwise,} \end{cases} \quad (\text{B3})$$

and $x(t)$ a d -dimensional stochastic process, which can be expressed as

$$\begin{aligned} x(t) - x(0) &= - \int_0^t \frac{d'(T-\tau)}{a(T-\tau)} x(\tau) d\tau + \int_0^t \sqrt{\frac{2D_0}{(n(\tau) + n_{\min})^\beta}} dB(\tau). \end{aligned} \quad (\text{B4})$$

Then, the solution of (B1) $u(x(t), n(t), p, t)$ satisfies the BSDE^{55,56}

$$\begin{aligned} &u(x(t), n(t), p, t) - g(x(t), n(t), p) \\ &= \int_t^T f(x(\tau), n(\tau), p, u(x(\tau), n(\tau), p, \tau)) d\tau - \int_t^T \sqrt{\frac{2D_0}{(n(\tau) + n_{\min})^\beta}} \nabla_x u(x(\tau), n(\tau), p, \tau) \cdot dB(\tau) \\ &\quad - \int_t^T \int_{\mathbb{Z} \setminus \{0\}} u(x(\tau), n(\tau-), p, \tau) - u(x(\tau), n(\tau-), p, \tau) \tilde{J}(d\tau, dn; n(\tau-)). \end{aligned} \quad (\text{B5})$$

2. Deep BSDE Method

Now, by resolving (B4) and (B5), we can obtain the solution of the corresponding original equation. We pay attention to the solution $u(x_0, n_0, p, 0)$, where $(x_0, n_0, p) \in \mathbb{N} \times \mathbb{R}^d \times \mathbb{R}^1$ has already been determined. The $u(x_0, n_0, p, 0) \approx \theta_\phi$ is treated as a parameter in the model, and the BSDE (B5) is considered as the way to get the value of u at the terminal time T when $u(x(0) = x_0, n(0) = n_0, p, 0)$ and $\nabla_x u(x(t), n(t), p, t)$ as

well as $u(x(t), n(t) \pm 1, p, t)$ are known, where $\nabla_x u(x, n, p, t)$ is approximated through a neural network

$$\nabla_x u(x, n, p, t) \approx \psi_1(x, n, p, t | \theta_{\psi_1}), \quad (\text{B6})$$

with parameters θ_{ψ_1} and $\delta_n^\pm u(x, n, p, t) = [u(x, n-1, p, t) - u(x, n, p, t), u(x, n+1, p, t) - u(x, n, p, t)]^T$ is approximated by a neural network

$$\delta_n^\pm u(x, n, p, t) \approx \psi_2(x, n, p, t | \theta_{\psi_2}), \quad (\text{B7})$$

with parameters θ_{ψ_2} . Given a division of the time interval $[0, t] : 0 = t_0 < t_1 < \dots < t_{N-1} < t_N = T$, we use the simple

Euler scheme for $k = 0, 1, \dots, N-1$ as

$$\begin{aligned}
 & x(t_{k+1}) - x(t_k) \\
 &= -\frac{a'(T-t_k)}{a(T-t_k)} x(t_k) \Delta t_k + \sqrt{\frac{2D_0}{(n(\tau) + n_{\min})^\beta}} \Delta B(t_k) \quad (\text{B8})
 \end{aligned}$$

and

$$\begin{aligned}
 & u(x(t_{k+1}), n(t_{k+1}), p, t_{k+1}) \\
 &= u(x(t_k), n(t_k), p, t_k) - f(x(t_k), n(t_k), p, u(x(t_k), n(t_k), p, t_k)) \Delta t_k + \sqrt{\frac{2D_0}{(n(t_k) + n_{\min})^\beta}} \nabla_x u(x(t_k), n(t_k), p, t_k) \cdot \Delta B(t_k) \quad (\text{B9}) \\
 &+ u(x(t_k), n(t_{k+1}), p, t_k) - u(x(t_k), n(t_k), p, t_k) - T_n u(x(t_k), n(t_k), p, t_k),
 \end{aligned}$$

where $\Delta t_k = t_{k+1} - t_k$, $\Delta B(t_k) = B(t_{k+1}) - B(t_k)$, and $n(t_{k+1}) - n(t_k)$ satisfies (B3).

We take the discretized time $\{t_k\}_{0 \leq k \leq N}$, frequency p , the randomly generated paths $\{n(t_k)\}_{0 \leq k \leq N}$, $\{x(t_k)\}_{0 \leq k \leq N}$, and $\{B(t_k)\}_{0 \leq k \leq N}$ as the input data of the neural net-

work. Letting $\theta = \{\theta_\phi, \theta_{\psi_1}, \theta_{\psi_2}\}$, the final output $\hat{u}(\{x(t_k), n(t_k), p, B(t_k), t_k\}_{0 \leq k \leq N} | \theta)$ is obtained through the scheme (B9) as an approximation of $g(x(T), n(T), p)$. The difference from the given terminal conditions is used to construct the loss function

$$\text{Loss}(\theta) = \mathbb{E} \left[|g(x(T), n(T), p) - \hat{u}(\{x(t_k), n(t_k), p, B(t_k), t_k\}_{0 \leq k \leq N} | \theta))|^2 \right]. \quad (\text{B10})$$

ACKNOWLEDGMENTS

This work was supported by the National Natural Science Foundation of China under Grant Nos. 12225107 and 12071195, the Major Science and Technology Projects in Gansu Province-Leading Talents in Science and Technology under Grant No. 23ZDKA0005, the Innovative Groups of Basic Research in Gansu Province under Grant No. 22JR5RA391, and Lanzhou Talent Work Special Fund.

REFERENCES

- ¹C. W. Gardiner, *Handbook of Stochastic Methods for Physics, Chemistry and Natural Sciences*, vol. 3 (Berlin: Springer, 2004).
- ²N. G. Van Kampen, *Stochastic Processes in Physics and Chemistry*, vol. 1 (Amsterdam: North-Holland, 1992).
- ³G. A. Pavliotis, *Stochastic Processes and Applications: Diffusion Processes, the Fokker-Planck and Langevin Equations*, vol. 60 (New York: Springer, 2014).
- ⁴S. B. Yuste, E. Abad, and C. Escudero, *Phys. Rev. E* **94**, 032118 (2016).
- ⁵F. Le Vol, E. Abad, and S. B. Yuste, *Phys. Rev. E* **96**, 032117 (2017).
- ⁶F. Le Vol and S. B. Yuste, *Phys. Rev. E* **98**, 042117 (2018).
- ⁷T. Zhou, P. B. Xu, and W. H. Deng, *J. Phys. A: Math. Theor.* **55**, 025001 (2021).
- ⁸T. Zhou, P. B. Xu, and W. H. Deng, *J. Stat. Phys.* **187**, 9 (2022).
- ⁹B. Wang, S. M. Anthony, S. C. Bae, and S. Granick, *PNAS* **106**, 15160 (2009).
- ¹⁰J. Guan, B. Wang, and S. Granick, *ACS Nano* **8**, 3331 (2014).
- ¹¹B. Wang, J. Kuo, S. C. Bae, and S. Granick, *Nat. Mater.* **11**, 481 (2012).

- ¹²V. Sposini, A. V. Chechkin, F. Seno, G. Pagnini, and R. Metzler, *New J. Phys.* **20**, 043044 (2018).
- ¹³M. A. dos Santos and L. M. Junior, *Chaos Solitons Fractals* **144**, 110634 (2021).
- ¹⁴C. Xue, X. Zheng, K. Chen, Y. Tian, and G. Hu, *J. Phys. Chem. Lett.* **7**, 514 (2016).
- ¹⁵K. C. Leptos, J. S. Guasto, J. P. Gollub, A. I. Pesci, and R. E. Goldstein, *Phys. Rev. Lett.* **103**, 198103 (2009).
- ¹⁶V. Berezinsky and A. Gazizov, *Astrophys. J.* **643**, 8 (2006).
- ¹⁷J. A. Peacock, *Cosmological Physics* (Cambridge: Cambridge University Press, 1999).
- ¹⁸B. Ryden, *Introduction to Cosmology* (Cambridge: Cambridge University Press, 2017).
- ¹⁹K. A. Landman, G. J. Pettet, and D. F. Newgreen, *Bull. Math. Biol.* **65**, 235 (2003).
- ²⁰E. J. Crampin, E. A. Gaffney, and P. K. Maini, *Bull. Math. Biol.* **61**, 1093 (1999).
- ²¹A. G. Cherstvy, O. Nagel, C. Beta, and R. Metzler, *Phys. Chem. Chem. Phys.* **20**, 23034 (2018).
- ²²P. Fried and D. Iber, *Nat. Commun.* **5**, 5077 (2014).
- ²³X. D. Wang and Y. Chen, *Phys. Rev. E* **107**, 024105 (2023).
- ²⁴Y. Chen, X. D. Wang, and W. H. Deng, *J. Stat. Phys.* **169**, 18 (2017).
- ²⁵W. H. Deng and E. Barkai, *Phys. Rev. E* **79**, 011112 (2009).
- ²⁶J. Bouchaud and A. Georges, *Phys. Rep.* **195**, 127 (1990).
- ²⁷R. Metzler and J. Klafter, *Phys. Rep.* **339**, 1 (2000).
- ²⁸L. R. Evangelista and E. K. Lenzi, *Fractional Diffusion Equations and Anomalous Diffusion* (Cambridge: Cambridge University Press, 2018).
- ²⁹Y. Chen, X. D. Wang, and W. H. Deng, *Phys. Rev. E* **99**, 042125 (2019).
- ³⁰Y. Chen, X. D. Wang, and W. H. Deng, *Phys. Rev. E* **99**, 012135 (2019).
- ³¹W. Sutherland, *Philos. Mag.* **9**, 781 (1905).
- ³²M. Von Smoluchowski, *Ann. Phys.-Berlin.* **326**, 756 (1906).
- ³³A. Einstein, *Investigations on the Theory of the Brownian Movement* (New York: Dover Publications, 1956).

This is the author's peer reviewed, accepted manuscript. However, the online version of record will be different from this version once it has been copyedited and typeset.

PLEASE CITE THIS ARTICLE AS DOI: 10.1063/5.0232075

- ³⁴T. J. Lampo, S. Stylianidou, M. P. Backlund, P. A. Wiggins, and A. J. S-pakowitz, *Biophys. J.* **112**, 532 (2017).
- ³⁵W. K. Chong, K. Thirumal, D. Giovanni, T. W. Goh, X. Liu, N. Mathews, S. Mhaisalkar, and T. C. Sum, *Phys. Chem. Chem. Phys.* **18**, 14701 (2016).
- ³⁶Y. Li, K. Suleiman, and Y. Xu, *Phys. Rev. E* **109**, 014139 (2024).
- ³⁷W. Wang, R. Metzler, and A. G. Cherstvy, *Phys. Chem. Chem. Phys.* **24**, 18482 (2022).
- ³⁸K. Suleiman, Y. Li, and Y. Xu, *J. Phys. A: Math. Theor.* **57**, 115002 (2024).
- ³⁹K. He, F. Babaye Khorasani, S. T. Retterer, D. K. Thomas, J. C. Conrad, and R. Krishnamoorti, *ACS Nano* **7**, 5122 (2013).
- ⁴⁰S. Hapca, J. W. Crawford, and I. M. Young, *J. R. Soc. Interface* **6**, 111 (2009).
- ⁴¹F. Baldovin, E. Orlandini, and F. Seno, *Front. Phys.* **7**, 124 (2019).
- ⁴²S. Nampoothiri, E. Orlandini, F. Seno, and F. Baldovin, *Phys. Rev. E* **104**, L062501 (2021).
- ⁴³S. Nampoothiri, E. Orlandini, F. Seno, and F. Baldovin, *New J. Phys.* **24**, 023003 (2022).
- ⁴⁴D. Boal, *Mechanics of the Cell* (Cambridge: Cambridge University Press, 2012).
- ⁴⁵S. Karlin and J. McGregor, *Trans. Amer. Math. Soc.* **86**, 366 (1957).
- ⁴⁶J. Medhi, *Stochastic Models in Queueing Theory* (Amsterdam: Academic Press, 2002).
- ⁴⁷M. Doi and S. F. Edwards, *The Theory of Polymer Dynamics*, vol. 73 (Oxford: Oxford University Press, 1988).
- ⁴⁸E. Yamamoto, T. Akimoto, A. Mitsutake, and R. Metzler, *Phys. Rev. Lett.* **126**, 128101 (2021).
- ⁴⁹X. D. Wang and Y. Chen, *Phys. A* **577**, 126090 (2021).
- ⁵⁰P. B. Xu, T. Zhou, R. Metzler, and W. H. Deng, *Phys. Rev. E* **101**, 062127 (2020).
- ⁵¹A. V. Chechkin, F. Seno, R. Metzler, and I. M. Sokolov, *Phys. Rev. X* **7**, 021002 (2017).
- ⁵²X. D. Wang and Y. Chen, *Phys. Rev. E* **106**, 024112 (2022).
- ⁵³X. D. Wang, Y. Chen, and W. H. Deng, *Phys. Rev. E* **98**, 052114 (2018).
- ⁵⁴J. Q. Han, A. Jentzen, and W. E, *PNAS* **115**, 8505 (2018).
- ⁵⁵H. Wang and W. H. Deng, *J. Mach. Learn.* **3**, 215 (2024).
- ⁵⁶T. Zhou, H. Wang, and W. H. Deng, *J. Phys. A: Math. Theor.* **57**, 285001 (2024).